Understanding the molecular role of syndecan-1 in the regulation of caspase-6 during the progression of cardiac arrhythmia

YUANCHU WU*, LIN CHEN* and CAIHONG WANG

Department of Cardiology, Affiliated Wujiang Hospital of Nantong University, Suzhou, Jiangsu 215200, P.R. China

Received June 16, 2020; Accepted June 24, 2021

DOI: 10.3892/etm.2021.10614

Abstract. The role of caspase-6 in heart disease is not well understood, particularly with respect to cardiac arrhythmia. Also, the function of syndecan-1 in the stimulation of inflammation or a regenerative response after cardiac injury is unclear. Leptin receptor-deficient (C57BL/KS-lepr^{db}/lepr^{db}) mice were used in the present study. In addition to developing type 2 diabetes, they also develop initial- and end-stage cardiac arrhythmia after 5 and 8 months, respectively. The initial and end-stage arrhythmias were confirmed through progressive variations in the PP intervals observable in electrocardiograms. Histopathological images of the cardiac tissue exhibited scattered and loosened cardiac cells at the initial stage of cardiac arrhythmia, whereas tissue hardness and extensive structural changes in cardiomyocytes were evident at the end stage. At the molecular level, the progressive upregulation of caspase-6 was observed as the cardiac arrhythmia progressed. In the initial stage of arrhythmia, immunohistochemistry revealed that caspase-6 was expressed at the surface of cardiac cells, suggesting that caspase-6 targeted the extracellular matrix, leading to a loosening of the cardiac tissue structure. In the end stage of cardiac arrhythmia, caspase-6 expression was abundant in the cytoplasm, as well as at the cell surface, suggesting that caspase-6 may have cleaved intermediate filaments, paving the way for cellular morphological changes and apoptosis. Notably, syndecan-1 was upregulated 5.8-fold in the initial stage of cardiac arrhythmia, but downregulated at the end stage. Syndecan-1 may restrict the expression of caspase-6 in the initial stage of cardiac arrhythmia, while its downregulation at the end stage may allow destructive changes via caspase-6 overexpression. Furthermore, the knockdown of syndecan-1 using small interfering RNA enhanced the expression of caspase-6 in the cardiac tissue by factors of 1.8 and 1.2 at the initial and end stages of cardiac arrhythmia, respectively, compared with that in non-silenced cardiac tissue. Therefore, it may be concluded that syndecan-1 plays a major role in the regulation of caspase-6 during the pathological stages of cardiac arrhythmia.

Correspondence to: Dr Caihong Wang, Department of Cardiology, Affiliated Wujiang Hospital of Nantong University, 2666 Ludang Road, Wujiang, Suzhou, Jiangsu 215200, P.R. China
E-mail: benjamin_w@163.com

*Contributed equally

Key words: cardiac arrhythmia, caspase-6, syndecan-1, C57BL/KS-lepr^{db}/lepr^{db}

Introduction

Cardiac arrhythmias leading to sudden cardiac death are a common health issue worldwide (1). Arrhythmia includes abnormal cardiac rhythm, such as bradyarrhythmia, atrial fibrillation and abnormal electrical signal conduction in cardiac tissue (2). Cardiac rhythm abnormalities tend to worsen with increasing age and are more prevalent among male Caucasians. Other risk factors include cardiac comorbidities, such as hypertension, diabetes and congestive heart failure (3). Atrial fibrillation is a common complication of silent hypertension, the inefficient management of which often leads to stroke (4). Improved therapies and updated treatments are urgently required to reduce the mortality associated with arrhythmias (5). Unfortunately, inadequate research into the progression of arrhythmias and the underlying mechanisms that link them with heart failure has hindered the efficiency of treatment (6).

To improve the understanding of arrhythmias, it is necessary to determine which genes are involved in the disturbance of electrophysiology and in the progression of arrhythmogenesis (7). Syndecan-1 is a transmembrane heparan sulfate proteoglycan that plays a major role in atherogenesis and cardiac fibrosis, mostly in association with angiotensin II (8). It is involved in the regulation of inflammation, response to injury, regeneration and remodeling, and is protective following myocardial infarction (9).

Generally, caspases are major influencers of inflammation and apoptosis (10). Caspase-6 acts as a substrate for numerous neuronal-associated proteins, some of the most important of which are microtubule-associated proteins (11). It has been reported that following its induction by tumor necrosis factor (TNF)-α, caspase-6 cleaves the cardiac intermediate filament desmin to initiate cardiac failure (12). In the present study, the aim was to determine the inductive role of syndecan-1 in the regulation of caspase-6 at different stages of

the development of cardiac arrhythmia. In the present study, Leptin receptor-deficient (C57BL/KS-lepr^{db}/lepr^{db}) mice were used, which normally develop type 2 diabetes, in addition to developing initial- and end-stage cardiac arrhythmia after 5 and 8 months, respectively.

Materials and methods

Experimental animals and study design. Leptin receptor-deficient male mice (13) (n=36; average 23 g; 2 months old) with an altered genetic background (C57BL/KS-lepr^{db}/lepr^{db}) were purchased from Jackson Laboratory. The mice were housed in a laboratory environment and carefully monitored until they were acclimated to the new environment (one week). The mice were maintained at 24˚C with relative humidity of 55-60%, with free access to water and regular chow and with a 12-h light/dark cycle. The genetically modified C57BL/KS-lepr^{db}/lepr^{db} mice (n=24) were maintained for 5 and 8 months (n=12 per time point) to develop initial and advanced stages of cardiac arrhythmia, respectively. The control C57BL/KS mice (n=12) were maintained under the same conditions, with the exception that they followed a regular diet throughout the experiments. At the end of 5 and 8 months, the animals (n=6) were sacrificed in each group by cervical dislocation and for control mice 8 month samples were taken for experimental analysis. Prior to sacrifice, the body weight and blood glucose level in a blood sample taken from the tail tip were measured. The cardiac weight was determined after sacrifice. The experimental procedure, animal handling, maintenance and protocol were pre-approved by and carried out according to the guidelines of the Ethics Committee of Affiliated Wujiang Hospital of Nantong University (ref. no. AWHNU06/04/18).

Electrocardiogram (ECG) analyses. To analyze their electrophysiological condition, the control and leptin receptor-deficient diabetic mice were subjected to ECG analysis, as previously described (14). In brief, the mice were anesthetized with 1% isoflurane vapor, and an ECG electrode needle was inserted subcutaneously in the upper right limb and lower left abdomen. The ECG was recorded until the signal returned to baseline and the heart rate was stable (maximum of 8 min). The average times between successive P waves (PP interval), from the onset of the P wave to the start of the QRS complex (PR interval) and between QRS complexes (RR interval) were determined from the ECGs.

Histology and immunohistochemistry. After sacrifice, the mouse heart was carefully excised by thoracotomy. The cardiac tissue was washed with 1X phosphate-buffered saline (PBS) and quickly transferred to 4% formalin solution for fixation at 37˚C for 48 h. Following fixation, the tissues were placed in increasing concentrations of isopropanol for dehydration. After clearing with xylene, the tissues were embedded with paraffin. The tissues were then sliced transversely using a microtome set to 6 μm. The sections were dewaxed with xylene, dehydrated with isopropanol and stained with hematoxylin (7 min) and eosin (20 sec) at room temperature for subsequent imaging using a Nikon light microscope (Eclipse Ei; Nikon Corporation). The cardiac tissue hardening and loosening were analyzed based on the cellular variations observed within the particular area.

For immunohistochemical analyses, the antigens were unmasked by boiling the sections for 10 min in 10 mM sodium citrate buffer (pH 6.0). Cellular endogenous peroxidase was blocked using methanol in 2% H_2O_2 for 20 min at 24˚C. After washing with 1X PBS, the non-specific sites in the sections were blocked using 4% bovine serum albumin (Sigma-Aldrich; Merck KGaA) in 1X Tris-buffered saline containing 0.1% Tween-20 (TBST) for 1 h at room temperature. The primary antibodies anti-syndecan-1 (ab128936; Abcam) and anti-caspase-6 (ab231349; Abcam) were added at 1:300 dilutions over the sections, which were kept at 4˚C for 5 h. The unbound antibody was washed away thrice with 1X Tris-buffered saline containing TBST and further incubated with a horseradish peroxidase (HRP)-conjugated secondary antibody (cat. no. ab205718; Abcam, 1:3,000 dilution) for 1 h at room temperature. The peroxidase signals, which indirectly reflect the binding of primary antibody, were visualized using a 3,3'-diaminobenzidine (DAB) kit (Sigma-Aldrich; Merck KGaA). The sections were counterstained with hematoxylin for 7 mins at room temperature, which gave a blue-purple hue to the background to contrast with the brown antibody signal under Nikon light microscope (Eclipse Ei; Nikon Corporation).

Silencing syndecan-1 using small interfering RNA (siRNA). Syndecan-1 expression was silenced using siRNA against syndecan-1 (siSyn; cat no. AM16708; Thermo Fisher Scientific, Inc.). The negative control used was a non-targeted siRNA with limited sequence similarity to the targeted gene (siCtr; cat no. AM4611; Thermo Fisher Scientific, Inc.). siRNA against GAPDH was also used (siGAPDH; cat no. AM4631; Thermo Fisher Scientific, Inc.) as a control, The siRNAs were suspended in water to a final concentration of 0.5 μg/μl. To facilitate the transfection, 0.5 μl 50 nM Lipofectamine® 2000 (Invitrogen; Thermo Fisher Scientific, Inc.) was mixed with the siRNA 20 min prior to injection. The control, initial- and late-stage cardiac arrhythmia groups were each divided into four groups as follows: Untreated, siCtr, siSyn and siGAPDH. Each group had six mice. The siRNA was injected into the tail veins of mice at the ages of 4 months (mice developing with initial-stage cardiac arrhythmia) or 7 months (mice developing with late-stage cardiac arrhythmia). The mice were sacrificed 1 month later (at the end of 5 and 8 months, respectively) and cardiac tissue samples were collected for analysis by western blotting.

Western blotting. The dissected heart was immediately placed in ice-cold 1X PBS and the right auricle tissue was used for protein sample preparation. The tissues were mechanically homogenized with ice-cold 2X Laemmli buffer (Bio-Rad Laboratories, Inc.). The homogenized tissue was then immediately heated in a boiling water bath for 5 min to release proteins from the cell lysate. The protein concentration in each sample was estimated using the Lowry method. The proteins were separated by SDS-PAGE (12% gel, 70 μg protein/well) for 4 h at 50 V. The separated proteins were then transferred to a polyvinyl difluoride membrane using the semi-dry transfer method. The membrane was blocked with 4% skimmed milk powder for 2 h at room temperature to prevent non-specific

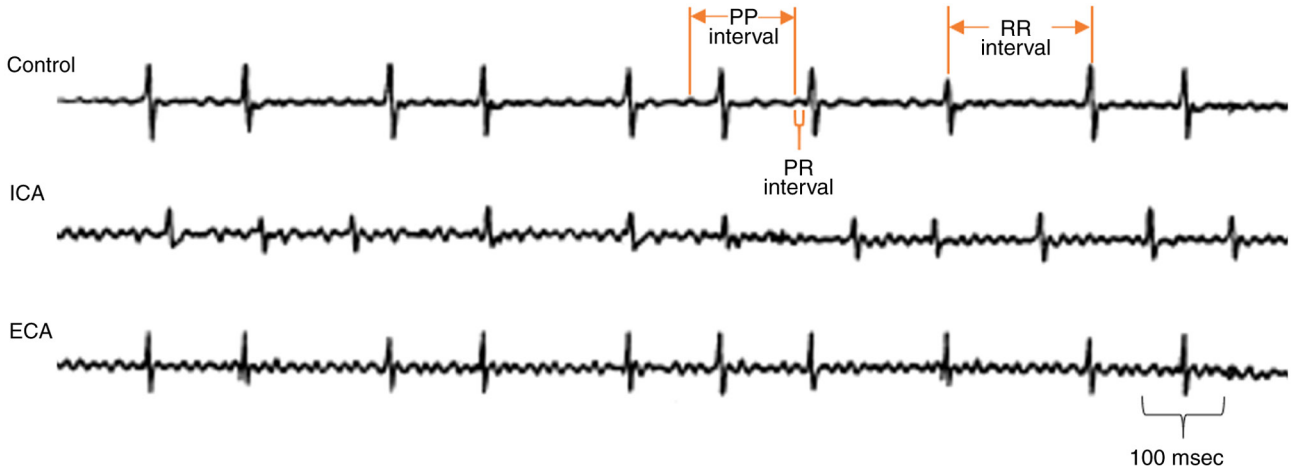

Figure 1. ECGs of leptin receptor-deficient mice at the initial and end stages of cardiac arrhythmia. The ECGs show progressive variation of the PP interval with increasing severity of cardiac arrhythmia, and variations in each beat, as evidenced by variable PP and PR intervals. ECGs, electrocardiograms; ICA initial-stage cardiac arrhythmia; ECA, end-stage cardiac arrhythmia; PP interval, average time between successive P waves; PR interval, average time from the onset of the P wave to the start of the QRS complex; RR interval, average time between QRS complexes.

binding, and the target proteins were detected by incubation for 4 h at 4˚C with the primary antibodies anti-syndecan-1 (cat. no. ab128936; Abcam; 1:1,000 dilution), anti-caspase-6 (cat. no. ab231349; Abcam; 1:500 dilution) and anti-β actin (cat. no. ab8227; Abcam; 1:1,000 dilution). Following gentle rocking for 5 min, the membrane was then incubated for 1 h at room temperature with goat anti-rabbit HRP-conjugated secondary antibody (ab6721; dilution, 1:4,000; Abcam). The membrane was washed thoroughly with 1X TBST buffer for 10 min and then counter reacted with DAB to obtain the protein signals. The intensity of the signal band was documented using Gel documentation system (InGenius3; Syngene) and analyzed using ImageJ software (v1.52h, National Institutes of Health).

Statistical analysis. The experiments or observations were performed at least three times, and the obtained data are presented as the mean ± standard deviation. The differences between two groups were compared using two-tailed Student's t-test and among multiple groups using two-way ANOVA followed by Tukey's post hoc tests for multiple comparisons. $P<0.05$ was considered to indicate a statistically significant result.

Results

Mouse model develops progressive cardiac arrhythmia. In comparison with the control mice, the leptin receptor-deficient mice exhibited abnormal weight gain with advancing age. The control C57BL/KS mice (n=12) exhibited an average mean weight of 30±2 g after 5 months and 34±2 g after 8 months. By comparison, the leptin receptor-deficient diabetic mice (n=12) exhibited mean weights of 41±3 g (37% higher than that of the control mice) after 5 months and 48±3 g after 8 months (41% higher than that of the control mice).

The leptin receptor-deficient mice were also hyperglycemic at 5 and 8 months. At 5 months, the control mice had fasting blood glucose levels of 80±4 mg/dl, while the leptin receptor-deficient diabetic mice had fasting blood glucose levels of 452±14 mg/dl. Similarly, at 8 months, the fasting blood glucose level of the leptin receptor-deficient mice was 517±16 mg/dl, while that of the control mice was 88±7 mg/dl.

The development of arrhythmia was monitored by the analysis of ECG recordings. The 5-month-old mice with leptin receptor deficiency exhibited longer PP intervals (120 msec) compared with the control mice (Fig. 1). Furthermore, the 8-month-old leptin receptor-deficient mice exhibited shorter and longer PP intervals more frequently, which directly reflect the development of adverse cardiac arrhythmia in the form of atrial fibrillation (Fig. 1). Furthermore, the PR and RR intervals exhibited progressive variations as the cardiac arrhythmia became severe (Fig. 1).

Histological analysis of initial and end stage cardiac arrhythmia. Cardiac specimens from the control, initial- and end-stage cardiac arrhythmic mice were sectioned and subjected to histopathological analysis (Fig. 2). The histomorphological analysis of the cardiac specimens from the control mice revealed elongated, branched cells with prominent nuclei (Fig. 2A). The 5-month-old leptin receptor-deficient mice exhibited histopathological changes that included scattered and loosened cardiac cells with enlarged, dark nuclei (Fig. 2B); after 8 months, when these mice had developed a severe form of cardiac arrhythmia, a complete change in cardiomyocyte structure was observed, with excessive secretion of extracellular matrix tissue leading to hardening of the tissue (Fig. 2C). These histological variations observed in the mice with initial- and end-stage cardiac arrhythmia were quantified and are graphically presented in Fig. 2D. The data indicate that cardiac tissue integrity progressed from a loosened cellular structure to tissue hardening as the cardiac arrhythmia progressed from initial- to end-stage (Fig. 2D).

Caspase-6 exhibits elevated expression in progressive stages of cardiac arrhythmia. Immunohistochemistry was used to analyze caspase-6 expression in the cardiac tissue of mice exhibiting initial- and end-stage arrhythmia. In the control cardiac tissue, caspase-6 was expressed at a low level (Fig. 3A). The expression of caspase-6 was markedly elevated at the

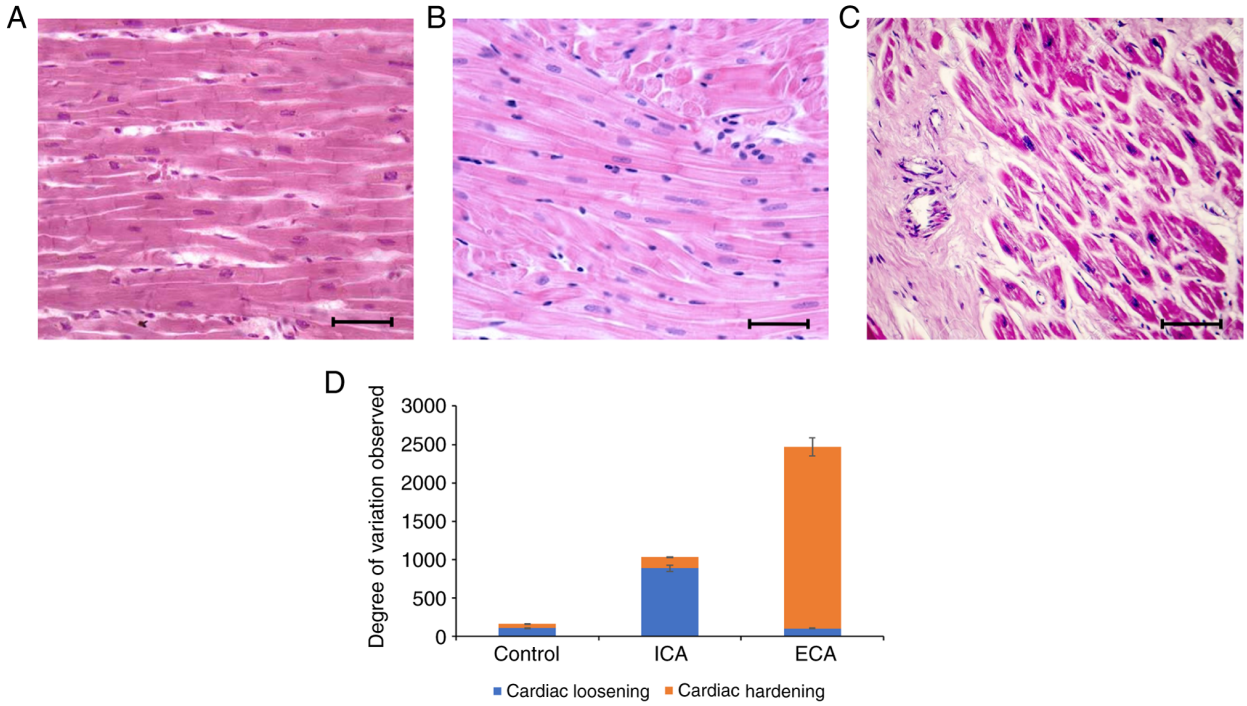

Figure 2. Histological variations in the cardiac tissue from mice at various stages of cardiac arrhythmia. (A) Normal mouse cardiac tissue, showing a compact cellular structure, with prominent nuclei. (B) Cardiac tissue from a mouse with ICA, showing a loosened cellular structure with a scattered appearance. (C) Cardiac tissue from a mouse with ECA, showing a complete change in cellular morphology, together with tissue hardening. Hematoxylin and eosin staining. Scale bar, 100 μm. (D) Graphical representation of histological variations observed in mouse cardiac tissue at the initial and end stages of cardiac arrhythmia compared with those of normal mice. ICA, initial-stage cardiac arrhythmia; ECA, end-stage cardiac arrhythmia.

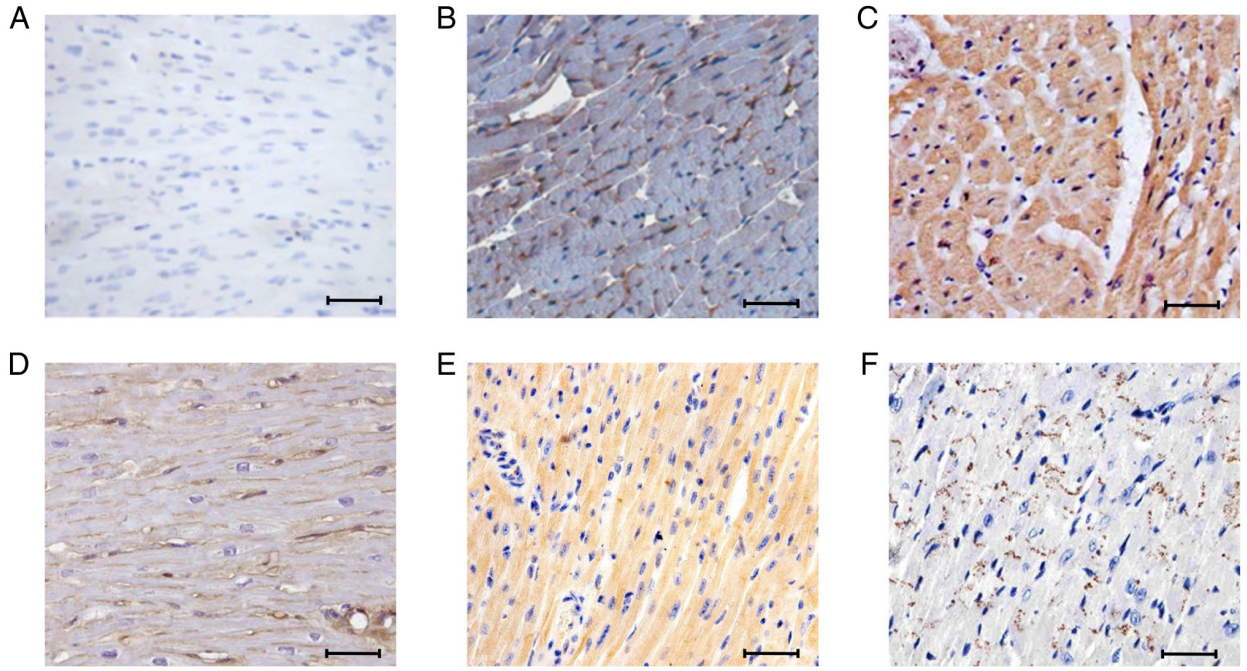

Figure 3. Immunohistochemical staining of caspase-6 and syndecan-1 in cardiac tissue from mice at various stages of cardiac arrhythmia. (A) Normal mouse cardiac tissue, showing very little caspase-6. (B) Cardiac tissue from a mouse in the initial stage of cardiac arrhythmia, showing caspase-6 expression on the cell surface. (C) Cardiac tissue from a mouse at an advanced stage of cardiac arrhythmia, showing abundant caspase-6 expression in the cytoplasm, as well as at the cell surface. (D) Normal mouse cardiac tissue, showing uniform limited expression of syndecan-1. (E) Cardiac tissue from a mouse in the initial stage of cardiac arrhythmia, showing extreme upregulation of syndecan-1. (F) Cardiac tissue from a mouse at an advanced stage of cardiac arrhythmia, showing decreased expression of syndecan-1. Scale bar, 100 μm.

initial stage of cardiac arrhythmia (Fig. 3B), and was elevated even further at the end stage of cardiac arrhythmia (Fig. 3C).

Syndecan-1 is induced in the initial stage of cardiac arrhythmia and repressed in the later stage. To understand

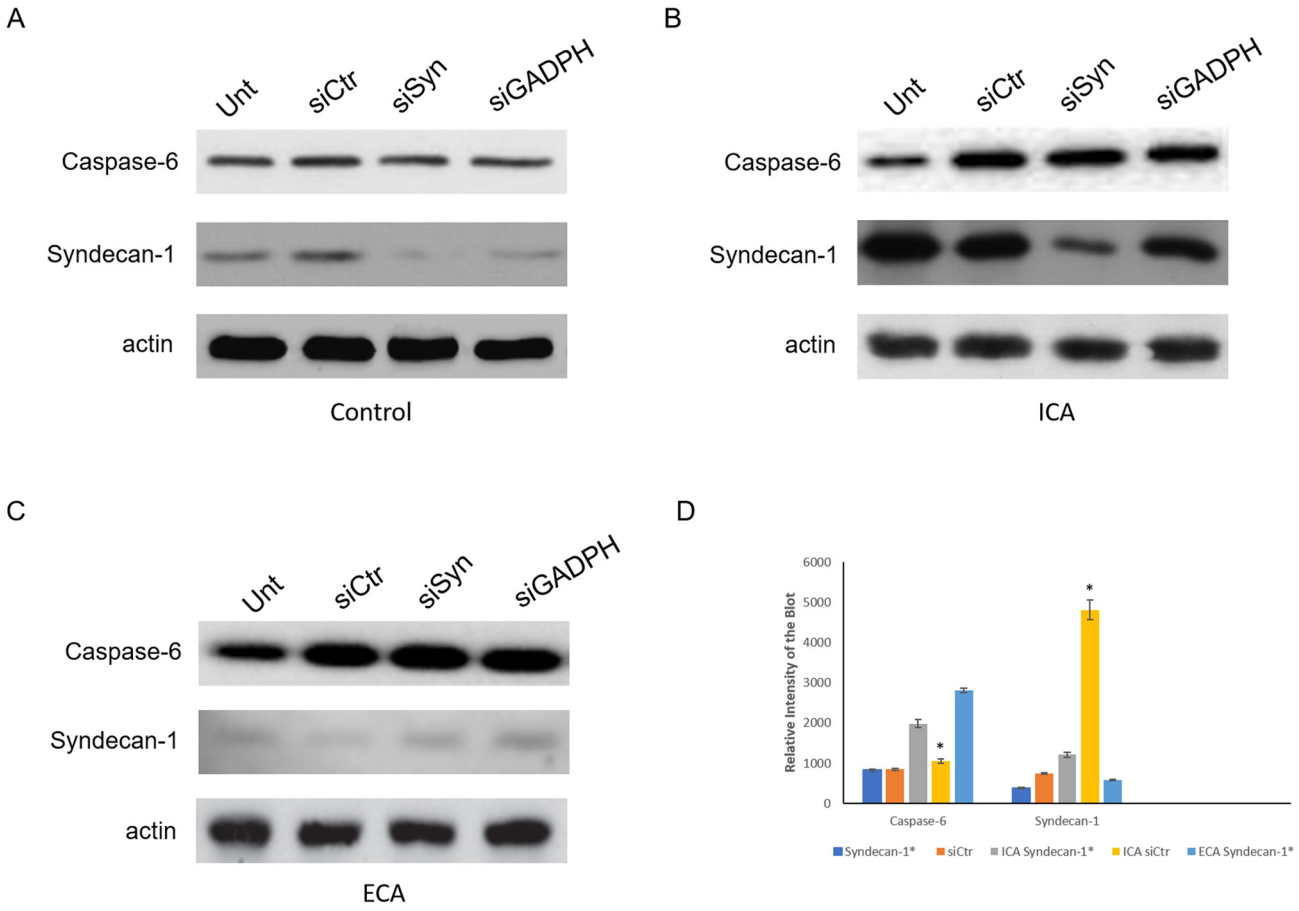

Figure 4. Western blots of the protein lysates of cardiac tissue from mice at various stages of cardiac arrhythmia. Expression of caspase-6 and syndecan-1 in cardiac tissue from the Unt, siCtr, siSyn and siGADPH groups of (A) control mice, (B) mice with ICA and (C) mice with ECA. (D) Quantification of caspase-6 and syndecan-1. *P<0.01. The results are normalized to the β-actin loading control. Unt, untreated; siCtr, control siRNA; siSyn, siRNA against syndecan-1; siGADPH, siRNA against GAPDH; siRNA, small interfering RNA; ICA, initial-stage cardiac arrhythmia; ECA, end-stage cardiac arrhythmia. *Represents the expression of caspase-6 or syndecan-1 in syndecan-1 silenced tissue.

the role of syndecan-1 in cardiac pathogenesis, immunohistochemical analyses of syndecan-1 expression were performed at progressive stages of cardiac arrhythmia (Fig. 3D-F). In the control cardiac tissue, syndecan-1 expression was observed primarily on cell surfaces (Fig. 3D). In cardiac tissues from the mice with initial-stage cardiac arrhythmia, syndecan-1 was expressed throughout the cardiac tissue with prominent expression on the cell surface and in the cytoplasm, which implies expression at the transcriptional level (Fig. 3E). However, syndecan-1 appeared to be downregulated in cardiac tissues from end-stage arrhythmic mice (Fig. 3F), relative to those from control mice (Fig. 3D).

Western blot analysis of caspase-6 and syndecan-1 in tissues from cardiac arrhythmic mice. Western blotting was also carried out to evaluate the expression of caspase-6 and syndecan-1 in the cardiac tissues of the mice (Fig. 4). In agreement with the immunohistochemistry data (Fig. 3), the expression of caspase-6 was observed to increase over the course of development of cardiac arrhythmia. In the cardiac tissues from the mice with initial-stage cardiac arrhythmia, the level of caspase-6 was 1.5-fold that of the control cardiac samples. Furthermore, in the cardiac tissues from the mice with end-stage cardiac arrhythmia, caspase-6 was expressed at 3.6-fold the level detected in control cardiac samples. Western blotting analysis also showed that syndecan-1 is extremely upregulated in the initial stage of cardiac arrhythmia, with 5.8-fold greater expression compared with that in the control samples. Surprisingly, however, syndecan-1 expression was reduced at the end stage of cardiac arrhythmia and was downregulated to almost half the level in the control cardiac tissue. In syndecan-1-silenced tissue at the initial stage of cardiac arrhythmia, the caspase-6 level was elevated to 1.8-fold that in the control siRNA treated group, while at the end stage, the caspase-6 level in the syndecan-1-silenced tissue was 1.2-fold that in the control siRNA treated group (Fig. 4). In this experiment, non-targeting siRNA served as a negative control and siRNA against GADPH served as an additional control.

Discussion

Leptin deficiency is associated with insulin-dependent metabolism, which affects cardiac rhythm, which in turn has chronotropic effects (15-17). Mice treated with streptozotocin also develop chronotropic responses, as well as type 1 diabetes mellitus (18). Since they are genetically modified, the leptin receptor-deficient C57BL/KS-lepr^{db}/lepr^{db}

mice provide more accurate experimental results than do streptozotocin-induced mice (13). In the present study, over the course of 5-8 months, the C57BL/KS-lepr^{db}/lepr^{db} mice exhibited increasing weight gain, elevated blood glucose levels and ECG abnormalities. A previous study showed that cardiac arrhythmia develops due to initial metabolic disturbances, which in turn affect cardioregulatory autonomic dysfunction (19). The present study is consistent with this finding. The results demonstrated that the heterogeneous pattern of ECG morphology became more complex over time; the PP interval and its uniformity was disturbed, indicating severe cardiac arrhythmia (20).

The histological data confirmed changes to the cellular morphology of the cardiac tissue, with a loosened structure appearing after 5 months. This loosened structure was likely due to unstable cellular adhesion components, resulting in the initiation of tissue remodeling and fibro-fatty replacement (21,22). After 8 months, the C57BL/KS-lepr^{db}/lepr^{db} mice exhibited cardiac tissue thickening, which was likely due to the infiltration of fat and/or fibrosis, affecting cardiac elasticity (23,24). The cardiac tissue hardening may also have been due to the excessive secretion of extracellular matrix to replace degenerated tissue (25). The risk factors for cardiac arrhythmia and heart dysfunction have been indicated to involve the excessive stimulation of extracellular matrix protein secretion, which leads to cardiac failure (26).

Caspase-6 has been associated with neurological disorders; it cleaves neuronal microtubule-associated proteins, causing neurodegeneration (27,28). Caspase-6 also plays a role in apoptosis, and its principal substrates are nuclear proteins and intermediate filaments (29). However, little is known about the role of caspase-6-mediated apoptosis in heart disease (30,31). In the present study, the elevated expression of caspase-6 in the cardiac tissue of the mice with initial- and end-stage cardiac arrhythmia may indicate that cardiac intermediate filaments and extracellular matrix were the targets of caspase-6 activity, which would disrupt the normal cardiac microarchitecture. In the initial stage of cardiac arrhythmia, the expression of caspase-6 occurred primarily at the cell surface, suggesting that disruption of the extracellular matrix was the initiating event leading to cardiac arrhythmia. Later in the progression of the arrhythmia, caspase-6 expression was observed inside the cells, as well as at the surface, suggesting that at the end stage, the intermediate filaments were also targeted. The increased level of caspase-6 expression in the cytoplasm may also be indicative of apoptosis (32). Indeed, caspase-6 has been associated with myocardial infarction and brain injury following cardiac arrest (33).

Syndecan-1 is reported to be a promising marker for the degree of cardiac fibrosis (34). In general, syndecan-1 is involved in the regulation of inflammation and regenerative responses, but its mode of action is highly variable and influenced by numerous independent factors such as liver fibrosis and growth stimulating conditions (9). In the present study, in the initial stage of cardiac arrhythmia, the expression of syndecan-1 was elevated and appeared to be protective by restricting caspase-6 expression. However, at the end-stage of cardiac arrhythmia, syndecan-1 was downregulated, favoring the overexpression of caspase-6 and the concomitant destruction of cardiac tissue.

In conclusion, the model C57BL/KS-lepr^{db}/lepr^{db} mice developed initial- and end-stage cardiac arrhythmia after 5 and 8 months, respectively. The overexpression of caspase-6 at the cell surface observed during the initial stage of arrhythmia suggests that caspase-6 initially targets the extracellular matrix. The later expression of caspase-6 within the cells suggests that the cytoskeleton is also targeted as the arrhythmia progresses. The overexpression of syndecan-1 in the initial stage of cardiac arrhythmia and its regenerative response suggests that syndecan-1 restricts the expression of caspase-6 in the initial stage, but then the downregulation of syndecan-1 favors the destructive overexpression of caspase-6 in the end-stage of cardiac arrhythmia.

Acknowledgements

Not applicable.

Funding

No funding was received.

Availability of data and materials

All data generated or analyzed during this study are included in this published article.

Authors' contributions

YW and CW contributed to the design of the study and fund mobilization. YW performed histology, immunohistochemistry, western blotting and silencing experiments and LC contributed to the experiments, CW performed the statistical analysis, critically reviewed the manuscript and provide support in the experiments. All authors read and approved the final manuscript. YW and CW confirm the authenticity of all the raw data.

Ethics approval and consent to participate

The experimental procedure, animal handling, maintenance and protocol were approved by the Ethics Committee of Affiliated Wujiang Hospital of Nantong University (ref. no: AWHNU06/04/18).

Patient consent for publication

Not applicable.

Competing interests

The authors declare that they have no competing interests.

References

1. Chugh SS, Roth GA, Gillum RF and Mensah GA: Global burden of atrial fibrillation in developed and developing nations. Glob Heart 9: 113-119, 2014.
2. Khurshid S, Choi SH, Weng LC, Wang EY, Trinquart L, Benjamin EJ, Ellinor PT and Lubitz SA: Frequency of cardiac rhythm abnormalities in a half million adults. Circ Arrhythm Electrophysiol 11: e006273, 2018.

3. Rietbrock S, Heeley E, Plumb J and van Staa T: Chronic atrial fibrillation: Incidence, prevalence, and prediction of stroke using the Congestive heart failure, Hypertension, Age> 75, Diabetes mellitus, and prior Stroke or transient ischemic attack (CHADS2) risk stratification scheme. Am Heart J 156: 57-64, 2008.
4. Abrich VA, Narichania AD, Love WT, Lanza LA, Shen WK and Sorajja D: Left atrial appendage exclusion during mitral valve surgery and stroke in atrial fibrillation. J Interv Card Electrophysiol 53: 285-292, 2018.
5. Wiseman T and Betihavas V: The association between unexplained falls and cardiac arrhythmias: A scoping literature review. Aust Crit Care 32: 434-441, 2019.
6. Zhang Y, Du W and Yang B: Long non-coding RNAs as new regulators of cardiac electrophysiology and arrhythmias: Molecular mechanisms, therapeutic implications and challenges. Pharmacol Ther 203: 107389, 2019.
7. Sinner MF, Tucker NR, Lunetta KL, Ozaki K, Smith JG, Trompet S, Bis JC, Lin H, Chung MK, Nielsen JB, *et al*: Integrating genetic, transcriptional, and functional analyses to identify 5 novel genes for atrial fibrillation. Circulation 130: 1225-1235, 2014.
8. Schellings MW, Vanhoutte D, van Almen GC, Swinnen M, Leenders JJ, Kubben N, van Leeuwen RE, Hofstra L, Heymans S and Pinto YM: Syndecan-1 amplifies angiotensin II-induced cardiac fibrosis. Hypertension 55: 249-256, 2010.
9. Miftode RS, Şerban IL, Timpau AS, Miftode IL, Ion A, Buburuz AM, Costache AD and Costache II: Syndecan-1: A review on its role in heart failure and chronic liver disease patients' assessment. Cardiol Res Pract 2019: 4750580, 2019.
10. Dagbay KB and Hardy JA: Multiple proteolytic events in caspase-6 self-activation impact conformations of discrete structural regions. Proc Natl Acad Sci USA 114: E7977-E7986, 2017.
11. Horowitz PM, Patterson KR, Guillozet-Bongaarts AL, Reynolds MR, Carroll CA, Weintraub ST, Bennett DA, Cryns VL, Berry RW and Binder LI: Early N-terminal changes and caspase-6 cleavage of tau in Alzheimer's disease. J Neurosci 24: 7895-7902, 2004.
12. Papathanasiou S, Rickelt S, Soriano ME, Schips TG, Maier HJ, Davos CH, Varela A, Kaklamanis L, Mann DL and Capetanaki Y: Tumor necrosis factor-α confers cardioprotection through ectopic expression of keratins K8 and K18. Nat Med 21: 1076-1084, 2015.
13. Soltysinska E, Speerschneider T, Winther SV and Thomsen MB: Sinoatrial node dysfunction induces cardiac arrhythmias in diabetic mice. Cardiovasc Diabetol 13: 122, 2014.
14. Sysa-Shah P, Sørensen LL, Abraham MR and Gabrielson KL: Electrocardiographic characterization of cardiac hypertrophy in mice that overexpress the ErbB2 receptor tyrosine kinase. Comp Med 65: 295-307, 2015.
15. Hasslacher C and Wahl P: Diabetes prevalence in patients with bradycardiac arrhythmias. Acta Diabetol Lat 14: 229-234, 1977.
16. Movahed MR, Hashemzadeh M and Jamal MM: Increased prevalence of third-degree atrioventricular block in patients with type II diabetes mellitus. Chest 128: 2611-2614, 2005.
17. Abenavoli T, Rubler S, Fisher VJ, Axelrod HI and Zuckerman KP: Exercise testing with myocardial scintigraphy in asymptomatic diabetic males. Circulation 63: 54-64, 1981.
18. Luo M, Guan X, Luczak ED, Lang D, Kutschke W, Gao Z, Yang J, Glynn P, Sossalla S, Swaminathan PD, *et al*: Diabetes increases mortality after myocardial infarction by oxidizing CaMKII. J Clin Invest 123: 1262-1274, 2013.
19. da Costa Goncalves AC, Tank J, Diedrich A, Hilzendeger A, Plehm R, Bader M, Luft FC, Jordan J and Gross V: Diabetic hypertensive leptin receptor-deficient db/db mice develop cardioregulatory autonomic dysfunction. Hypertension 53: 387-392, 2009.
20. Rawles JM, Pai GR and Reid SR: A method of quantifying sinus arrhythmia: Parallel effect of respiration on P-P and P-R intervals. Clin Sci (Lond) 76: 103-108, 1989.
21. Delmar M and McKenna WJ: The cardiac desmosome and arrhythmogenic cardiomyopathies: From gene to disease. Circ Res 107: 700-714, 2010.
22. Basso C, Czarnowska E, Della Barbera M, Bauce B, Beffagna G, Wlodarska EK, Pilichou K, Ramondo A, Lorenzon A, Wozniek O, *et al*: Ultrastructural evidence of intercalated disc remodelling in arrhythmogenic right ventricular cardiomyopathy: An electron microscopy investigation on endomyocardial biopsies. Eur Heart J 27: 1847-1854, 2006.
23. Sen-Chowdhry S, Morgan RD, Chambers JC and McKenna WJ: Arrhythmogenic cardiomyopathy: Etiology, diagnosis, and treatment. Annu Rev Med 61: 233-253, 2010.
24. MacKenna DA, Vaplon SM and McCulloch AD: Microstructural model of perimysial collagen fibers for resting myocardial mechanics during ventricular filling. Am J Physiol 273: H1576-H1586, 1997.
25. Khan R and Sheppard R: Fibrosis in heart disease: Understanding the role of transforming growth factor-beta in cardiomyopathy, valvular disease and arrhythmia. Immunology 118: 10-24, 2006.
26. Travers JG, Kamal FA, Robbins J, Yutzey KE and Blaxall BC: Cardiac fibrosis: The fibroblast awakens. Circ Res 118: 1021-1040, 2016.
27. Guo H, Albrecht S, Bourdeau M, Petzke T, Bergeron C and LeBlanc AC: Active caspase-6 and caspase-6-cleaved tau in neuropil threads, neuritic plaques, and neurofibrillary tangles of Alzheimer's disease. Am J Pathol 165: 523-531, 2004.
28. Albrecht S, Bogdanovic N, Ghetti B, Winblad B and LeBlanc AC: Caspase-6 activation in familial Alzheimer disease brains carrying amyloid precursor protein or presenilin i or presenilin II mutations. J Neuropathol Exp Neurol 68: 1282-1293, 2009.
29. Godefroy N, Foveau B, Albrecht S, Goodyer CG and LeBlanc AC: Expression and activation of caspase-6 in human fetal and adult tissues. PLoS One 8: e79313, 2013.
30. Nevière R, Fauvel H, Chopin C, Formstecher P and Marchetti P: Caspase inhibition prevents cardiac dysfunction and heart apoptosis in a rat model of sepsis. Am J Respir Crit Care Med 163: 218-225, 2001.
31. Qiu L and Liu X: Identification of key genes involved in myocardial infarction. Eur J Med Res 24: 22, 2019.
32. Parrish AB, Freel CD and Kornbluth S: Cellular mechanisms controlling caspase activation and function. Cold Spring Harb Perspect Biol 5: a008672, 2013.
33. Krajewska M, Rosenthal RE, Mikolajczyk J, Stennicke HR, Wiesenthal T, Mai J, Naito M, Salvesen GS, Reed JC, Fiskum G and Krajewski S: Early processing of Bid and caspase-6,-8,-10,-14 in the canine brain during cardiac arrest and resuscitation. Exp Neurol 189: 261-279, 2004.
34. Lunde IG, Herum KM, Carlson CC and Christensen G: Syndecans in heart fibrosis. Cell Tissue Res 365: 539-552, 2016.